TECHNIQUES *by D.G. Linzell, R.T. Leon, and A.H. Zureick*

INSTRUMENTATION PLANNING AND VALIDATION FOR FULL-SCALE BRIDGE TESTING

Large-scale testing to verify structural performance and develop design guidelines is common in civil engineering applications. The vast majority of these tests are conducted on individual structural elements with boundary conditions that simulate idealized frictionless roller or fixed supports. In addition to being economical from a testing standpoint, idealized boundary conditions are useful because they make comparisons to analytical models possible. However, realistic boundary conditions that incorporate loading eccentricities, friction at supports, connection slip, connection restraint, and non-fixed (relative) bracing are important in assessing the behavior of redundant structures. An example of such structures is a curved steel plate girder bridge. These bridges exhibit a complex geometry with girders constructed from slender plate elements susceptible to buckling. Typical I-shape plate girder cross-sections can also be relatively weak in torsion during erection due to lack of external bracing, resulting in large deformations. During the construction of a curved steel plate girder bridge, loading and restraint conditions can change several times, as the structure changes from a pair of individual steel girders interconnected by few cross frames and bracing members to a multi-girder system interconnected by a rigid floor slab and numerous cross frames and bracing members. To design and reasonably assess their performance, it is necessary to resort to advanced analytical tools that can track the deformations and forces for the entire structural system during the construction process. This paper describes a unique large-scale test on a curved I-girder bridge model in which the forces and deformations were monitored throughout the construction process. The emphasis is on describing the background and compromises needed to test such a complex system, on discussing the steps taken to ensure the reliability of the data collected and on providing information related to correctly planning and executing large-scale experimental studies.

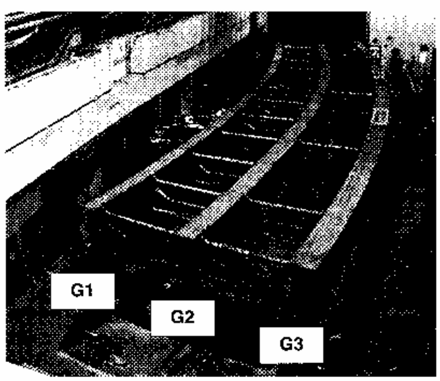

Fig. 1: Experimental curved bridge structure

DESCRIPTION OF TEST STRUCTURE

Existing design rules for horizontally curved steel bridges are generally based on research conducted in the 1960s and 1970s. These rules are constrained by the available test data and are considered very conservative for many common design situations today. To address these shortcomings, the Federal Highway Administration (FHWA) began the Curved Steel Bridge Research Project (CSBRP) in 1992. The main objective of the project was to revise and expand the American Association of State Highway and Transportation Officials (AASHTO) *Guide Specifications for Horizontally Curved Bridges* (1980, 1993) currently governing the design of curved bridges in the United States. The experimental portion of the project centered on testing several full-scale curved plate I-girder sections as parts of a test frame that simulated many characteristics of a real bridge. Full-scale tests were deemed essential because past experimental work involved only 1/20-scale to 1/2-scale system models where full similitude could not be maintained. Detailed discussions of past experimental and analytical curved steel bridge research and its shortcomings can be found in References 4, 5 and 3.

The experimental bridge structure that was the focal point of the CSBRP tests is shown in Figs. 1 and 2. It consists of a 27.4 m (90 ft.) long, simply-supported, three-girder system. The bridge was supported on spherical bearings that permitted translation in both the radial and tangential directions of the girders. Stability of the system was achieved by connecting girder G2 to an external frame on the left end and restraining the radial movement of both bearings on girder G2.

The three-girder system was proportioned so that different plate girder specimens could be spliced into the middle 1/8th

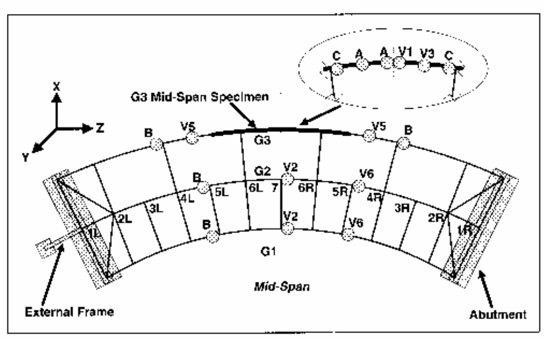

Fig. 2: Instrumented girder section schematic

D.G. Linzell (SEM Member) is an Assistant Professor at Penn State University, University Park, PA. R.T. Leon (SEM Member) and A.H. Zureick are Professors at The Georgia Institute of Technology, Atlanta, GA.

portion of the outside girder (G3) and tested to their ultimate flexural strength in a frame that provided realistic loading and boundary conditions. The rest of the structure (i.e. the interior girders, G2 and G1, and all radial cross frames (CF) and lower lateral bracing (LLB) members) was designed to remain elastic through the duration of the loading (Hall, 1994). This permitted an economical and efficient examination of the limit states of a series of full-scale plate girders with differing proportions.

The girders were approximately 1270 mm (50 in.) deep, with flanges ranging in width from 406 to 610 mm (16 to 24 in.) and in thickness from 19 to 30 mm (3/4 to 1-3/16 in.). The webs were 1219 mm (48 in.) deep, with thicknesses varying from 8 to 13 mm (5/16 to 1/2 in.). The tubes making up the cross-frames were 127 mm (5 in.) in diameter, with 6 mm (1/4 in.) wall thickness. The entire bridge assembly weighed approximately 535 kN (120 kips), and was loaded with six point loads, one near each of the third points of the three girders. Given the required number of actuators and their capacities along with the need to avoid over-constraining deformations, each test was completed in load-control using a series of small load increments.

INSTRUMENTATION

Initially, the main limitation on instrumentation was the number of available channels in the existing data acquisition systems (DAS). The total number of available channels was slightly over 800, but they were distributed among eight separate systems. These systems offered a wide range of inputs, signal conditioning capabilities and scanning rates, but could neither communicate with one another to synchronize readings nor accommodate placing inputs into a single database. Shortly after testing, three of the original DAS were replaced with a newer system that, in addition to providing extensive alarm, signal conditioning and processing capabilities, also added 200 channels. Thus at the initiation of testing, DAS capabilities totaled approximately 1000 channels with approximately 800 channels being integrated into a single system. Many of the decisions made at the earliest stages of instrumentation planning were driven by extensive finite element modeling. These models, analyzed using ABAQUS, contained as many as 50000 DOF and utilized the full nonlinear material and geometric features available in the program. The analytical studies were completed both to design the frame and the test sections as well as to aid instrumentation planning.

From an experimental standpoint, instrumentation planning was guided by two principal objectives. The first objective was to obtain reliable data from the G3 mid-span specimens throughout the loading history. This required that the girder G3 be extensively instrumented (Figs. 2 and 3) so that all relevant force components could be quantified. Sections labeled A, B and C in Fig. 3 corresponded to the locations shown in Fig. 2 and consisted primarily of quarter bridge resistance strain gages. To monitor strains, from which stresses were obtained, during the construction period (about 3 months) and to avoid the use of long cables that could interfere with erection, approximately 90 vibrating wire strain gages were installed (sections V1 to V6 in Fig. 2). These sections contained entirely vibrating wire gages or

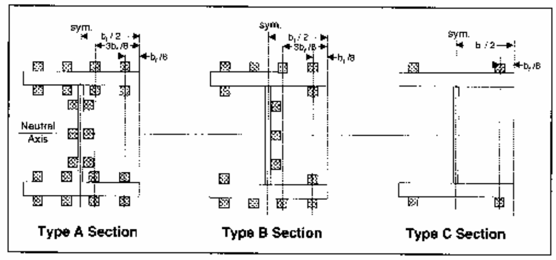

Fig. 3: Location of resistance strain gages at instrumented sections A, B and C

a combination of vibrating wire and resistance gages and they were placed onto the girder cross section in similar fashion to the resistance-gaged sections shown in Fig. 3 (i.e. V1, V3, V5 corresponded to A; V2, V6 corresponded to B). During erection, these vibrating wires gages were monitored with portable dataloggers and they were connected to a fixed DAS shortly before testing began.

Given the critical nature of these data, duplicate measurements were desirable. However, the limit on available channels prevented a significant number of duplicate measurements from being taken. In their place, extensive software-based cross-checking of the data was implemented during and after each test to assess repeatability (i.e., the gages at each cross-section gave a reasonable distribution of strains in both the elastic and inelastic range). Robustness of the data was assessed primarily by comparing internal and external forces and moments as computed from data recorded from the instrumentation. These calculations were carried out for several free-body diagrams (i.e., mid portion of G3 only, G3 only, half the bridge and others) to provide cross-checks on the readings. Extensive material tests on coupons from plates making up the main girders accompanied the full-scale testing so that yielding and strain hardening stress levels could be determined. Numerical integration of computed stresses at strain gage locations in each cross-section then allowed for calculation of the total internal forces acting on that cross-section. Software checks permitted elimination of strain gages from a section calculation once the gage had ceased to function or exceeded its output range.

Vertical external loads and reactions were recorded using full-bridge, high capacity flat load cells. Each girder rested on Teflon coated bearing plates that developed small but important tangential and radial horizontal reactions. To measure reactions in these three principal directions at each support (i.e. vertical, tangential and radial), the load cell assembly shown in Fig. 4 was devised and calibrated. The design involved four instrumented studs mounted to an outer steel retainer ring and to a circular steel plate, termed a "puck", located within that ring. Injected between the "puck" and bearing plate on which it rested was a layer of grease, which rendered this surface practically frictionless. Calibration of these assemblies was performed using simultaneous combinations of vertical loads and horizontal loads from hydraulic actuators. Tests performed during construction of the experimental structure required intermediate girder shoring

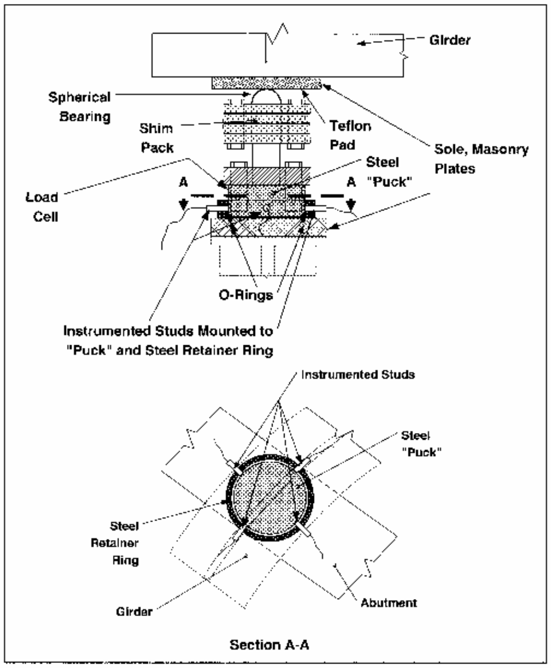

Fig. 4: Load cell assembly

and 9 additional load cells were used to monitor reactions at the shoring points.

During testing, it was also necessary to monitor strains in the rest of the test frame to ensure that no yielding occurred except within the G3 mid-span specimens and that forces at the ends of the G3 test segments were known. To ensure reusability of the frame, any yielding of the test frame outside G3 had to be prevented. Given the degree of redundancy of the structure, this required a number of careful preliminary analyses as the locations of stress concentrations were not necessarily obvious. To ensure that forces at the ends of the G3 segments were known, it was necessary to instrument at least four of the five individual cross frame members (Fig. 5). There were 13 cross frames (1R-6R, 1L- 6L, and 7 in Fig. 2) between G1 and G2 and 8 cross frames (1R, 2R, 4R, 6R, 1L, 2L, 4L and 6L) between G2 and G3. Those frames could experience a combination of biaxial bending, axial, and torsional forces, which means the number of

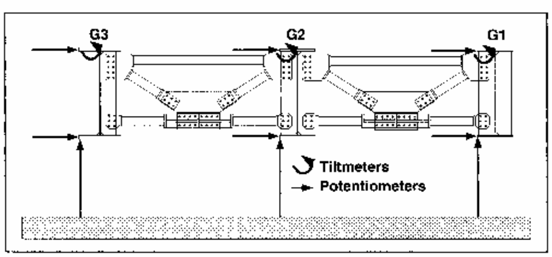

Fig. 5: Mid-span deformation instrumentation

strain gages required to characterize such behavior was potentially very large. After a series of component tests (detailed in the next section), tubular sections were selected in order to reduce the required number of sensors.

Vertical and radial deformations (e.g., translations and rotations) were monitored using a combination of conventional wire potentiomenters, LVDTs, and tiltmeters at mid-span (Fig. 5), the third points and the supports of each of the three girders. In addition, deformations at the top flanges of all three girders and deformations on the web and bottom flanges of G3 and the G3 mid-span specimens were monitored using 131 fixed targets. These targets were acquired using a Coherent Bridge Laser Measurement System (CBLM) that could perform rapid surface scans or locate and track individual targets in space at a slower rate. The time required to acquire and measure individual target three-dimensional displacements was considerable, as changes in geometry from one testing step to another varied widely from target to target. Thus, the CBLM was used only at select instances during testing.

During construction, a total of 1023 independent instrument inputs were used, consisting of: 673 resistance strain gages; 94 vibrating wire strain gages; 21 load cells; 12 instrumented studs; 39 LVDTs and potentiometers; 14 tiltmeters; 131 CLBM targets; and 39 total station targets.

EQUILIBRIUM CALCULATIONS

Calculations to verify equilibrium of forces and moments about all three principal axes were conducted. The equilibrium calculations for forces about the Y axis (vertical) and moments about the X axis (about the strong axis of the plate girder) were generally simple and gave consistent results. Calculation of forces about the X and Z axes (radial and transverse) were less accurate as the forces on the bearings in the radial and transverse directions were relatively small in comparison with those in the vertical direction. The calculations of moment equilibrium about the Y and Z axes (about weak axis and torsion) were problematic because large distances between the supports and the critical girder sections amplified the errors.

Equilibrium calculations required the measurement of internal forces in the radially oriented cross frames between the girders. The final cross frame design consisted of five tubular members arranged in a K-type frame (Fig. 5). To minimize the number of gages required, a series of component tests was carried out on circular sections similar to those used in the bracing members. The test setup and instrumentation for these studies are shown in Fig. 6. Individual cross frame member tests investigated two possible instrumentation schemes: one which involved a combination of full and quarter bridge strain gage circuits and one which used only quarter bridge inputs with numerical manipulation being employed in the DAS to determine axial, bending and twisting effects. The major trade-off between the two schemes was that the first required many more gages but produced higher resolution outputs. A representative comparison of results in the elastic range is shown in Fig. 7. The results show very good agreement for the range between about 2% of the maximum load (Lower Bound) and up to the

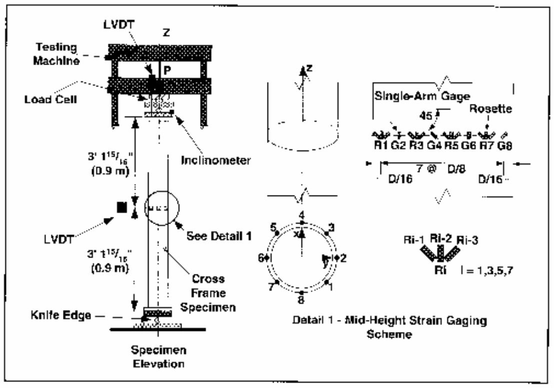

Fig. 6: Representative cross frame member test elevation and details

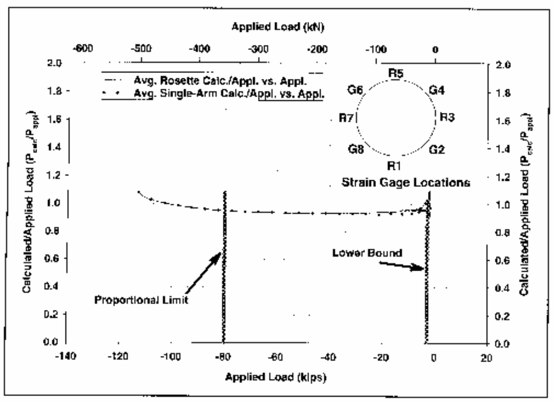

Fig. 7: Representative comparison of average calculated to applied axial loads, cross frame member testing

initiation of yielding (Proportional Limit). Results from the comparisons indicated that four single-arm resistance strain gages, mounted at 90° intervals around the tubular member's periphery and along its longitudinal axis, would reasonably permit estimation of internal axial loads and bending moments about orthogonal local axes passing through the gages. This configuration required approximately 400 resistance strain gages on the cross frame members for each G3 mid-span specimen test.

DATA VALIDATION

Robustness of the measurements was validated through extensive monitoring during the construction phase and through elastic cycling prior to initiating each G3 mid-span specimen test. Since establishing overall equilibrium required taking moments (forces times distances) about different points in the structure, and since these distances were quite large (sometimes in excess of 30 m), small changes in forces could lead to substantial changes in equilibrium calculations. A series of Monte Carlo simulations were performed to examine the sensitivity of select equilibrium calculations to cumulative variations in strains recorded from cross frame members for one particular construction test. The first Monte Carlo simulation evaluated the accuracy of equilibrium calculations for the inside girder (G1) assuming normal distributions with a standard deviation of 3.87 $\mu\varepsilon$ from actual test data. Simulations were then conducted with strain gage standard deviations increased to 5, 10 and 20 $\mu\varepsilon$. Moment equilibrium results from those simulations are shown in Table 1. It shows that, while adjustments in the variability of gage strain readings did not appreciably affect mean equilibrium calculations, they had great influence on standard deviations in equilibrium results that could be obtained. When slight increases in strain gage variability were introduced, standard deviations for corresponding moment equilibrium calculation values increased by a factor of ten. This indicated that equilibrium was quite sensitive to cumulative variations in strain gage readings that were within the instruments' resolution ranges. The components that exhibited the largest increases in standard deviations, the moments about the X and Y-axes (Fig. 2), were those that were heavily influenced by cross frame member forces and by the distances through which those forces acted.

The accuracy of equilibrium calculations for various free-body diagrams of the structure was assessed by normalizing results for each force and moment component being examined. They were normalized with respect to total positive contributions that resulted from all external and internal forces acting on the free-body diagram. So that normalization would be made to consistent totals, the time step during testing that produced the largest forces onto the free-body being studied was used as the normalizing parameter.

A representative equilibrium accuracy assessment plot is shown in Fig. 8. Each testing step represented a change in support conditions for the structure (i.e. removal or replacement of an intermediate shoring support frame). An example of the normalization procedure can be demonstrated for moment about the global X-axis, M_x, which was oriented about the radial direction (Fig. 2). After X-axis moment equilibrium sums were normalized against the maximum positive total to M_x for that free-body diagram, results indicated that equilibrium errors were less than 1% of the total positive moment contribution about the X-axis during the test. Although not shown in Fig. 8, certain comparisons showed equilibrium sums that were 10 percent to 20 percent of the total. These comparisons initiated modifications to original instrument placement and positioning schemes and helped identify malfunctioning instruments and acquisition equipment. They also indicated that: (1) equilibrium calculations were sensitive to cumulative changes in strain readings from the cross frames; (2) zeroing instruments at the beginning of a test may introduce larger errors than actually existed; (3) shutting off data acquisition systems overnight introduced a shift in equilibrium results that was caused by cooling of the systems and instruments and settlement of the structure; and (4) equilibrium checks required for evaluation of bending specimen behavior in the inelastic range, when some crucial instruments may be out- of-range and ineffective, were shown to provide acceptable results.

CONCLUSIONS

Instrumentation planning was essential for the Curved Steel Bridge Research Project (CSBRP) given the size of the struc-

Table 1—Moment Equilibrium Monte Carlo Simulation Means and Standard Deviations

COMPONENT	MONTE CARLO SIMULATION	EQUILIBRIUM SUMMATION MEAN kN-m (k-ft)	EQUILIBRIUM SUMMATION STANDARD DEVIATION kN-m (k-ft)
M_x	Raw Data	91.3 (67.2)	6.4 (4.7)
	Gage SD = 5 $\mu\varepsilon$	91.1 (67.0)	18.3 (13.5)
	Gage SD = 10 $\mu\varepsilon$	90.8 (66.8)	26.9 (36.6)
	Gage SD = 20 $\mu\varepsilon$	90.1 (66.2)	73.3 (53.9)
M_y	Raw Data	44.1 (31.7)	53.5 (39.3)
	Gage SD = 5 $\mu\varepsilon$	41.6 (30.6)	106.9 (78.6)
	Gage SD = 10 $\mu\varepsilon$	38.5 (28.3)	213.9 (157.3)
	Gage SD = 20 $\mu\varepsilon$		
M_z	Raw Data	−28.7 (−21.1)	1.0 (0.7)
	Gage SD = 5 $\mu\varepsilon$	28.7 (−21.1)	2.6 (1.9)
	Gage SD = 10 $\mu\varepsilon$	28.7 (·21.1)	5.2 (3.8)
	Gage SD = 20 $\mu\varepsilon$	−28.6 (−21.0)	10.4 (7.6)

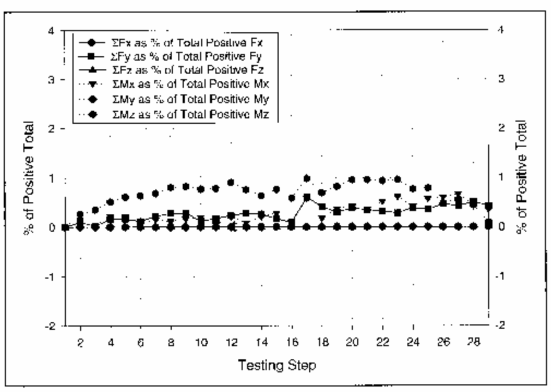

Fig. 8: Representative construction testing equilibrium accuracy assessment plot

ture and associated costs. This planning involved preliminary analytical and experimental studies of individual bridge components and portions of the final structure during construction. The validation studies conducted during construction provided confidence in the final results and led to a successful completion of the project.

REFERENCES

1. American Association of State Highway and Transportation Officials (1980, 1993), *Guide Specifications for Horizontally Curved Bridges*.

2. Hall, D.H (1994), "Curved Girders Are Special," Proceedings of the 50th Anniversary Conference, SSRC, Lehigh University, pp. 101–115.

3. Linzell, D.G. (1999), "Studies of a Full-Scale Horizontally Curved Steel I-Girder Bridge System Under Self-Weight," Ph.D. Dissertation, School of Civil and Environmental Engineering, Georgia Institute of Technology.

4. Zureick, A., Naqib, R., and Yadlosky, J.M. (1994), "Curved Steel Bridge Research Project, Interim Report I: Synthesis," HDR Engineering, Inc., Publication Number FHWA-RD-93-129, December.

5. Zureick, A., and Naqib, R. (1999), "Horizontally Curved Steel I-Girders State-of-the-Art Analysis Methods," *ASCE Journal Bridge Engineering*, February, v4, n1, pp. 38–47. ■